

**UNIVERSIDAD SAN FRANCISCO DE QUITO USFQ**

**Colegio de Ciencias e Ingenierías**

**Acoustic Fluidized Bed Hydrodynamics Simulation**  
**Proyecto de investigación**

**Rafael Alejandro Granda Neto**

**Ingeniería Mecánica**

Trabajo de titulación presentado como requisito  
para la obtención del título de  
Ingeniero Mecánico

Quito, 19 de diciembre de 2017

UNIVERSIDAD SAN FRANCISCO DE QUITO USFQ  
COLEGIO DE CIENCIAS E INGENIERÍA

HOJA DE CALIFICACIÓN  
DE TRABAJO DE TITULACIÓN

Acoustic Fluidized Bed Hydrodynamics Simulation

**Rafael Alejandro Granda Neto**

Calificación:

Nombre del profesor, Título académico

David Escudero, PhD

Firma del profesor

---

Quito, 19 de diciembre de 2017

## Derechos de Autor

Por medio del presente documento certifico que he leído todas las Políticas y Manuales de la Universidad San Francisco de Quito USFQ, incluyendo la Política de Propiedad Intelectual USFQ, y estoy de acuerdo con su contenido, por lo que los derechos de propiedad intelectual del presente trabajo quedan sujetos a lo dispuesto en esas Políticas.

Asimismo, autorizo a la USFQ para que realice la digitalización y publicación de este trabajo en el repositorio virtual, de conformidad a lo dispuesto en el Art. 144 de la Ley Orgánica de Educación Superior.

Firma del estudiante: \_\_\_\_\_

Nombres y apellidos: Rafael Alejandro Granda Neto

Código: 00108914

Cédula de Identidad: 0604244186

Lugar y fecha: Quito, 19 de diciembre de 2017

## Resumen

En este estudio se llevan a cabo simulaciones por computadora del comportamiento hidrodinámico de un reactor de lecho fluidizado acústico. Mediante el uso del programa Comsol Multiphysics se implementó un modelo computacional en dos dimensiones (2D) del reactor en el cual se determinaron los efectos de la frecuencia y el nivel de presión de sonido en las características hidrodinámicas del lecho fluidizado. El correcto acoplamiento de los módulos de Acústica y CFD de Comsol, permitieron validar el modelo computacional con previos resultados experimentales. Las simulaciones se llevaron a cabo en un modelo de un reactor de lecho fluidizado de 10.2 cm de diámetro lleno de cáscara de nuez molida, con una densidad de material de  $1440 \text{ kg/m}^3$ , y rangos de partículas entre 80 y  $212 \text{ }\mu\text{m}$ . La frecuencia; utilizada como fuente acústica se fijó en 200 Hz con un nivel de presión de sonido de 110 dB para la cáscara de nuez molida. Los resultados finales de las simulaciones muestran que el lecho fluidizado bajo la presencia de un campo acústico proporciona una fluidización más uniforme. Así, la intervención acústica afecta al comportamiento hidrodinámico local del lecho fluidizado.

Palabras clave: Simulación, CFD, Acústica, Lecho fluidizado, Hidrodinámica.

## Abstract

In this study, computer simulations are performed to study the hydrodynamic behavior of an acoustic fluidized bed reactor. By using Comsol Multiphysics software, a two-dimensional (2D) computational model of the reactor was implemented in which the effects of frequency and sound pressure level on the hydrodynamic characteristics of the fluidized bed were determined. The correct coupling of Comsol's Acoustics and CFD modules allowed to validate the computational model with previous experimental results. The simulations were carried out in a 10.2 cm diameter fluidized bed model filled with ground walnut shell, with a material density of  $1440 \text{ kg/m}^3$ , and particle ranges between 80 and 212  $\mu\text{m}$ . The frequency, used as an acoustic source, was set at 200 Hz with a sound pressure level of 110 dB for ground walnut shell. The final results of the simulations showed that the fluidized bed under the presence of an acoustic field provides a more uniform fluidization. Thus, the acoustic intervention affects the local hydrodynamic behavior of the fluidized bed.

Key Words: Simulation, CFD, Acoustics, Fluidized bed, Hydrodynamics.

## Table of Contents

<b>Resumen .....</b>	<b>4</b>
<b>Abstract .....</b>	<b>5</b>
<b>Table of Contents .....</b>	<b>6</b>
<b>List of Tables .....</b>	<b>7</b>
<b>List of Figures .....</b>	<b>8</b>
<b>Abbreviations .....</b>	<b>9</b>
<b>Introduction .....</b>	<b>10</b>
<b>Methodology .....</b>	<b>14</b>
CFD and Acoustics modules in Comsol Multiphysics .....	14
Hydrodynamic and Acoustic Model .....	15
Numerical Method and Simulation .....	18
<b>Results and Discussion .....</b>	<b>25</b>
Qualitative Results .....	25
Quantitative Results .....	30
Comparison with Experimental Results .....	35
<b>Conclusions .....</b>	<b>40</b>
<b>References .....</b>	<b>41</b>

## List of Tables

<b>Table 1.</b> Parameter values in the numerical simulations .....	23
<b>Table 2.</b> Meshing parameters .....	24

## List of Figures

<b>Figure 1.</b> Acoustic fluidized bed reactor used experimentally .....	16
<b>Figure 2.</b> Fluidized bed reactor model implemented in Comsol Multiphysics .....	17
<b>Figure 3.</b> Solid concentration for (a) 80 $\mu\text{m}$ , (b) 150 $\mu\text{m}$ and (c) 212 $\mu\text{m}$ ground walnut shell .....	26
<b>Figure 4.</b> Solid concentration map for 212 $\mu\text{m}$ ground walnut shell with acoustic coupling .....	27
<b>Figure 5.</b> Solid concentration maps for (a) $t = 1\text{s}$ , (b) $t = 2\text{s}$ , (c) $t = 3\text{s}$ , (d) $t = 4\text{s}$ and (e) $t = 5\text{s}$ .....	29
<b>Figure 6.</b> Solid concentrations at a height of 2.5 cm for (a) 80 $\mu\text{m}$ , (b) 150 $\mu\text{m}$ and (c) 212 $\mu\text{m}$ .....	31
<b>Figure 7.</b> Solid concentrations at a height of 2.5 cm for 212 $\mu\text{m}$ at $t = 5\text{s}$ .....	33
<b>Figure 8.</b> Solid concentrations at a height of 2.5 cm for (a) CFD and (b) Multiphysics at $t = 5\text{s}$ .....	34
<b>Figure 9.</b> Qualitative comparison between (a) experimental data (gas holdup) and (b) numerical results (solids concentration) for 212 $\mu\text{m}$ walnut shell .....	36
<b>Figure 10.</b> Quantitative comparison between (a) experimental data (gas holdup), (b) numerical results (acoustics) and (c) numerical results (no acoustics) for 212 $\mu\text{m}$ walnut shell .....	38



## Abbreviations

### ***Nomenclature***

$D$	bed diameter, m
$d$	particle diameter, m
$g$	gravity acceleration, $m/s^2$
$H$	static bed height, m
$I$	intensity vector, $W/m^2$
$P$	pressure, Pa
$t$	time, s
$U_{mf}$	minimum fluidization velocity, m/s
$\mathbf{u}$	velocity field, m/s
$\mathbf{u}_{slip}$	slip velocity, m/s
$\nabla p_s$	solid pressure, Pa

### ***Greek letters***

$\mu$	dynamic viscosity, $Pa \cdot s$
$\tau$	viscous stress tensor, Pa
$\rho$	density, $kg/m^3$
$\emptyset$	phase volume fraction
$\beta$	drag force coefficient, $kg/m^3s$
$\gamma$	ratio between specific heats

### ***Subscripts***

$c$	continuous phase
$d$	dispersed phase
$max$	maximum
$mf$	minimum fluidization

## Introduction

Fluidized bed reactors are devices in which a fluidization process takes place. In this process, a vertical upward current of fluid (liquid, gas or a mixture of both) is used to suspend solids in the form of particles. Commonly, these solid particles are referred to as the solid or dispersed phase and during fluidization they behave like a fluid. These reactors are used in a wide variety of industrial, chemical and pharmaceutical processes mainly because they allow high heat and mass transfer rates, uniform temperature distributions and low pressure drops. The complex gas-solid flow behavior in fluidized beds makes flow modeling a challenging task. Several assisted fluidization techniques have been proposed in order to overcome the limitations and to improve their intrinsic performance such as mechanical vibration, gas injection, pulsating flow, electric field, magnetic field and acoustic excitation (Khosravi Bizhaem & Basirat Tabrizi, 2017).

Sound-assisted fluidized beds have been studied for different Geldart type particles (Geldart type A - C) to understand the effects produced by the acoustic field on the fluidization behavior. This is an alternative and important option because it is a noninvasive technique that could influence and improve the bed hydrodynamic structure without affecting the properties of the bed material (Escudero & Heindel, 2013). The fluidization of cohesive, fine-grained powders can be enhanced by applying low-frequency and high-intensity sonic energy. Shuai et al. (2011) reported this improvement experimentally since homogeneous fluidization of fine particles has been achieved when operated in an acoustic field with appropriate combinations of bed weight and sound intensity and frequency.

When characterizing the hydrodynamic structure of a multiphase flow system, two main parameters are used; gas holdup or void fraction and the minimum fluidization velocity. In a fluidized bed, the gas holdup is defined as the volumetric gas fraction within the bed material (Escudero & Heindel, 2014). On the other hand, the minimum fluidization velocity is the superficial gas velocity at which the solid particles are just suspended in the fluidizing medium, and is a parameter that depends on the fluid properties, material properties and bed geometry (D. Escudero & Heindel, 2013). The presence of an acoustic field in a fluidized bed reactor produces a better fluidization quality which means an enhancement in the gas-solid mixing and a reduction in the minimum fluidization velocity.

Theoretical and numerical studies using computer simulations have allowed to analyze and better understand the hydrodynamic characteristics present in fluidized bed reactors. Computational Fluid Dynamics (CFD) approaches for modeling fluidized beds have been developed to a good level of maturity over the past three decades, primarily based on the kinetic theory of granular flows (Cloete, Johansen, & Amini, 2014). With the development of better technologies and the increase in the computing capacity of current systems, new theories and numerical approaches have emerged when modeling and simulating fluidized bed reactors. A few simulation researches have been carried out for studying slugging fluidized beds, mainly based on the Eulerian-Eulerian or two fluid model (TFM). The Lagrangian-Eulerian or discrete element model (DEM) has also become a useful tool to study the hydrodynamic behavior of gas-solid fluidized bed reactors (Wu, Ouyang, Yang, Li, & Wang, 2012).

In general, the hydrodynamics of multiphase flow systems can be described by two classes of models, namely the Euler-Lagrange and Euler-Euler models. In the Euler-

Lagrange models, the fluid phase is treated as a continuum, while the solid particles are tracked individually by solving Newton's second law of motion (Wu et al., 2012). On the other hand, Euler-Euler models assume the gas and solid phase as continuous and interpenetrating phases, which means that the equations used are the generalization of the Navier Stokes equations for interacting continua (Fan, 2006). Although both approaches are used in theoretical and numerical studies of these gas-solid systems, the Euler-Lagrange model is computationally more expensive and is not recommended when the concentrations of the solid phase are high. It is for this reason that the Euler-Euler model is widely used because is computationally more efficient and allows the simulation of large scale reactors and with the possibility of having high concentrations of solids.

More recent studies have concentrated on the simulation and analysis of acoustic fluidized bed reactors, which has allowed to compare and validate these numerical models with experimental results. Bizhaem and Tabrizi (2017) investigated the gas-solid flow behavior in a pulsed fluidized bed using the Eulerian-Eulerian two fluid model approach in conjunction with the kinetic theory of granular flow using particle sizes of Geldart A/B group. In this investigation the effect of various pulsation frequencies on the bed expansion ratio, solid volume fraction and solid axial velocity was discussed. Previous studies have also investigated the effect of gas pulsation on the flow pattern in 2D fluidized bed reactors. It has been found that pulsating flow with either a sinusoidal or square pattern improves the quality of fluidization inside a gas-solid fluidized bed reactor. A pulsating airflow improved the mixing of fine cohesive particles and reduced the minimum fluidization velocity using a wide range of pulsation amplitudes and frequencies (Shah, Utikar, & Pareek, 2017).

Most of the simulations of the hydrodynamic characteristics in an acoustic fluidized bed have been carried out using one dimensional (1D) models, some in two dimensions (2D), and using commercial software packages such as Ansys Fluent and The Multiphase Flow with Interphase eXchanges (MFIX) code. Comsol Multiphysics is a software package based on the finite element method that has been recently used for simulations of fluidized bed reactors assisted by pulsating flow, magnetic field, electric field, and very few with acoustic excitation in the form of acoustic vibrations. The goal of this study is to investigate the hydrodynamic behavior of an acoustic fluidized bed by carrying out 2D modeling with Comsol Multiphysics.

Multiphase fluid research studies have developed models using the computational fluid dynamics method in order to investigate the hydrodynamics of acoustic fluidized beds. The challenge of this project is to determine the effects of frequency and sound pressure level in the hydrodynamics of a fluidized bed. The coupling of the CFD module with the acoustics one will allow the modeling of the acoustic fluidized bed reactor using solid particles of Geldart type A and B, the solution of the governing equations and obtaining results of the hydrodynamic behavior of the system, including solid concentration profiles inside the bed, which will be validated with experimental results obtained by Escudero (2014).

## Methodology

### CFD and Acoustics modules in Comsol Multiphysics

#### *CFD Module*

Computational fluid dynamics is an integral part of a large number of processes that occur in all branches of engineering. Its range of application is so diverse and wide that it would be almost impossible not to use this tool when modeling and simulating any of these processes. The CFD module in Comsol enables the user to model laminar and turbulent single-or multiphase flow along with solvers and meshes that are optimized for fluid-flow applications and have built-in stabilization methods (Comsol, 2015).

This module offers a large number of options that allow the modeling of complex systems and processes in which, in addition to the flow of some type of fluid, phenomena that involve heat transfer or chemical reactions are present. With the physics interfaces, it is possible to simulate laminar and turbulent flow, isothermal and non-isothermal flow, Newtonian and non-Newtonian flow, multiphase flow and also flow in porous media (Comsol, 2015). The user interface in each of the existing submodules of the CFD module has a large number of tools and settings that include predetermined shapes and figures for the design of the system that is being modeled, to a series of different domains, boundary conditions, parameters of the model and properties of the fluid, which facilitate a close approximation to the real model to be simulated.

#### *Acoustics Module*

The acoustics module of Comsol enables you to model sound waves in any type of medium, either under the presence of a liquid or gas and even solid materials that can

be represented as porous materials if the application requires it. The capabilities and functionality of this module solves problems in the general areas of acoustics such as, vibrations, pressure and elastic waves, acoustic-structure interaction, thermoacoustics and aeroacoustics (Comsol, 2015). Many of the current engineering systems involve the presence of acoustic phenomena that influence their performance. Understanding the way in which these acoustic effects influence these systems and processes is of great interest since they are present in simple elements such as an exhaust pipe to very complex devices such as aircraft turbines.

When it is necessary to model and analyze the propagation, emission, radiation and diffraction of sound in any type of geometry, the acoustics module offers a wide variety of options and together with the possibility of coupling several physics in the same study, it becomes a very powerful tool to carry out simulations. This module supports frequency domain, modal and transient studies for fluid flow as well as frequency, eigenfrequency, transient and static analyses when the problem to be solved involves structures (Comsol, 2015).

### **Hydrodynamic and Acoustic Model**

Fluidized bed reactors are multiphase flow systems in which the principles of conservation of mass, momentum and energy are applied; this approach is based on the basis of the local average technique (Zhang, Zhang, & Zhang, 2003). In the present simulations, the Euler-Euler two fluid model was used to simulate the hydrodynamic behavior of the fluidized bed. In the Eulerian-Eulerian approach, both phases are treated as interpenetrating continua where the governing equations for both phases are solved, and the additional equations (which arise due to the dispersed phase), are

modelled using the kinetic theory of granular flow (KTGF) (Patro, 2014). At the time of modelling the fluidized bed with the Euler-Euler model, it is necessary to define a volume fraction or solids concentration.

In order to make a comparison of the experimental data with the results obtained through the simulations, the complete system of the fluidized bed was modeled, that is, the acoustic source was added to the original system, which for this specific case used a loudspeaker located in the upper part of the reactor, as shown in figure 1.

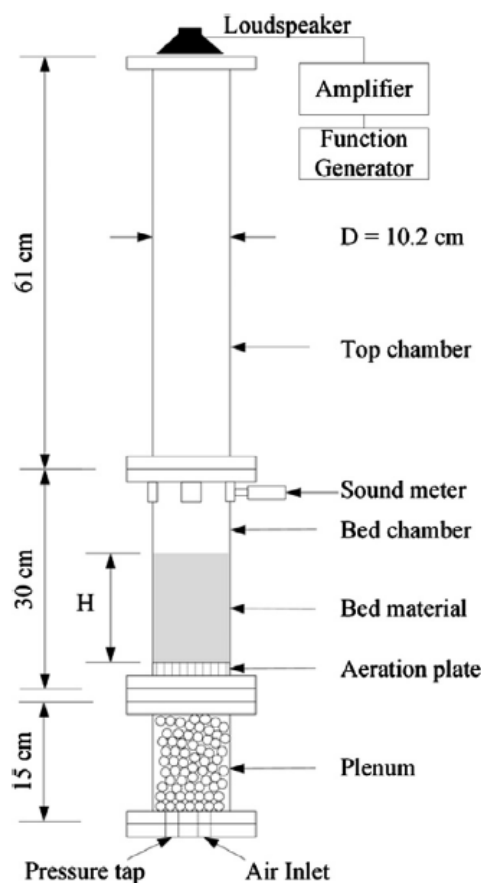


**Figure 1. Acoustic fluidized bed reactor used experimentally (Escudero, 2014)**

In the simulations carried out in this study, two physics interfaces available in Comsol Multiphysics were used: The Euler-Euler model (described previously) which belongs to the multiphase flow branch of the CFD module and the Linearized Euler model, which



can be found in the aeroacoustics branch of the acoustics module. The linearized Euler model is used to compute the acoustic variations in density, pressure and velocity in the presence of a background mean-flow that is well approximated by an ideal gas flow. The linearized Euler equations used by this physics interface are the linearized continuity, momentum, and energy equations, which are solved in the time domain (Comsol, 2015).

In this study, a 2D computational model of a gas-solid acoustic fluidized bed is implemented in Comsol Multiphysics. The fluidizing material is ground walnut shell ( $\rho_{\text{walnut shell}} = 1440 \text{ kg/m}^3$ ) with three different particle diameters (80  $\mu\text{m}$ , 150  $\mu\text{m}$  and 212  $\mu\text{m}$ ). The hydrodynamic and acoustic model of the reactor (figure 2) is simulated with an acoustic source, in which a frequency of 200 Hz with a sound pressure level of 110 dB are used for the ground walnut shells.

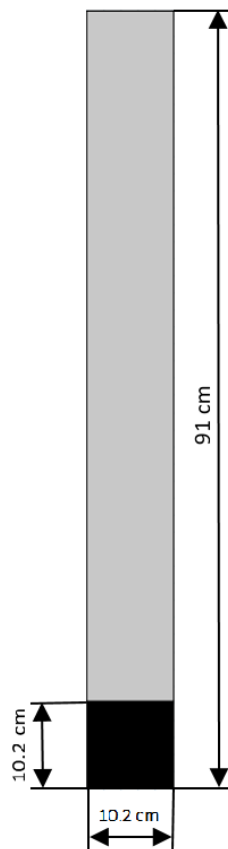


**Figure 2. Fluidized bed reactor model implemented in Comsol Multiphysics**

## Numerical Method and Simulation

### *Numerical Method*

In order to simulate the hydrodynamic behavior of the fluidized bed, the governing equations of the Euler-Euler two fluid model are solved. In Comsol Multiphysics, the Euler-Euler model, laminar flow interface solves two sets of Navier-Stokes equations, one for each phase (continuous phase and dispersed phase), in order to calculate the velocity field for each phase (Comsol, 2015). The interchange of momentum between the phases is described by a drag model, a transport equation is used to track the volume fraction of the solid phase and the pressure is computed from a mixture-averaged continuity equation (Comsol, 2015).

Assuming no mass transfer between the phases, the following continuity equations stand for the continuous and dispersed phases:

$$\frac{\partial}{\partial t}(\rho_c \phi_c) + \nabla \cdot (\rho_c \phi_c \mathbf{u}_c) = 0 \quad (1)$$

$$\frac{\partial}{\partial t}(\rho_d \phi_d) + \nabla \cdot (\rho_d \phi_d \mathbf{u}_d) = 0 \quad (2)$$

Where the following relation accounting for the phases volume fractions has to be fulfilled:

$$\phi_c = 1 - \phi_d \quad (3)$$

The momentum equations are written having in consideration one continuous phase and one dispersed phase (Comsol, 2015):

$$\rho_c \phi_c \left[ \frac{\partial}{\partial t}(\mathbf{u}_c) + \mathbf{u}_c \nabla \cdot (\mathbf{u}_c) \right] = -\phi_c \nabla p + \nabla \cdot (\phi_c \boldsymbol{\tau}_c) + \phi_c \rho_c \mathbf{g} + \mathbf{F}_{m,c} + \phi_c \mathbf{F}_c \quad (4)$$

$$\rho_d \phi_d \left[ \frac{\partial}{\partial t}(\mathbf{u}_d) + \mathbf{u}_d \nabla \cdot (\mathbf{u}_d) \right] = -\phi_d \nabla p + \nabla \cdot (\phi_d \boldsymbol{\tau}_d) + \phi_d \rho_d \mathbf{g} + \mathbf{F}_{m,d} + \phi_d \mathbf{F}_d \quad (5)$$

Where the viscous stress tensors for both phases are as follows:

$$\boldsymbol{\tau}_c = \mu_c \left( \nabla \mathbf{u}_c + (\nabla \mathbf{u}_c)^T - \frac{2}{3} (\nabla \cdot \mathbf{u}_c) \mathbf{I} \right) \quad (6)$$

$$\boldsymbol{\tau}_d = \mu_d \left( \nabla \mathbf{u}_d + (\nabla \mathbf{u}_d)^T - \frac{2}{3} (\nabla \cdot \mathbf{u}_d) \mathbf{I} \right) \quad (7)$$

The dynamic viscosities of the two interpenetrating phases have default values which are equal to a simple mixture viscosity (Krieger type model) (Comsol, 2015):

$$\mu_c = \mu_d = \mu_{\text{mix}} = \mu_c \left( 1 - \frac{\phi_d}{\phi_{d,\text{max}}} \right)^{-2.5\phi_{d,\text{max}}} \quad (8)$$

In the Euler-Euler model, the drag force is represented by the following relation (Comsol, 2015):

$$\mathbf{F}_{\text{drag},c} = -\mathbf{F}_{\text{drag},d} = \beta \mathbf{u}_{\text{slip}} \quad (9)$$

Where the slip velocity is defined as:

$$\mathbf{u}_{\text{slip}} = \mathbf{u}_d - \mathbf{u}_c \quad (10)$$

When setting up the CFD model, a solid pressure model must be set. In the present simulations, the predefined solid pressure model of Gidaspow and Ettehadieh was used (Comsol, 2015):

$$\nabla p_s = -10^{-8.76\phi_c + 5.43} \nabla \phi_c \quad (11)$$

The fully coupled multiphysics system of the acoustic fluidized bed reactor was achieved by adding the acoustic excitation into the Euler-Euler model. To do so, the

governing equations present in the linearized Euler interface are solved in the time domain (transient).

The following linearized Euler equations assume the fluid to be an ideal gas which is the common approach in the literature (Comsol, 2015):

$$\frac{\partial \rho}{\partial t} + \nabla \cdot (\rho \mathbf{u}_0 + \rho_0 \mathbf{u}) = S_c \quad (12)$$

$$\frac{\partial \mathbf{u}}{\partial t} + \nabla \cdot \left( \mathbf{u} \mathbf{u}_0 + \frac{p}{\rho_0} \mathbf{I} \right) + \frac{p}{\rho_0} (\mathbf{u}_0 \cdot \nabla) \mathbf{u}_0 - p \nabla (\rho_0^{-1}) + (\nabla \mathbf{u}_0 - (\nabla \cdot \mathbf{u}_0) \mathbf{I}) \mathbf{u} = S_m \quad (13)$$

$$\frac{\partial p}{\partial t} + \nabla \cdot (\gamma p_0 \mathbf{u} + p \mathbf{u}_0) + (1 - \gamma) (\mathbf{u} \cdot \nabla) p_0 - (1 - \gamma) (\nabla \cdot \mathbf{u}_0) p = S_c \quad (14)$$

Where the ratio between the specific heats at constant pressure and constant volume is defined as:

$$\gamma = \frac{C_p}{C_v} \quad (15)$$

Finally, the instantaneous intensity vector is expressed as follows (Comsol, 2015):

$$\mathbf{I}_i = (p_0 \mathbf{u} + p \mathbf{u}_0) \left( \frac{p}{\rho_0} + \mathbf{u}_0 \cdot \mathbf{u} \right) + \rho \mathbf{u}_0 T s \quad (16)$$

### ***Simulation***

In previous investigations, researchers observed some differences between three-dimensional and two-dimensional axisymmetric calculated void fraction in gas-solid flows. Nevertheless, 2D model was recommended to reduce computational time while maintaining the accuracy (Khosravi Bizhaem & Basirat Tabrizi, 2017). In this study, a 2D model of a fluidized bed reactor was implemented in Comsol Multiphysics. The simulations were performed at transient condition with a total time of simulation of 5

seconds. The dispersed phase used were solid particles of ground walnut shell with particle diameters of 80  $\mu\text{m}$ , 150  $\mu\text{m}$  and 212  $\mu\text{m}$ . Air was used as the continuous phase of the model. When simulating the fully coupled system of the acoustic fluidized bed, the acoustic field was added represented by a loudspeaker with a frequency of 200 Hz and a sound pressure level of 110 dB.

In the present simulations, the following are the initial and boundary conditions used in the Euler-Euler model for the CFD analysis:

- Initially, solid and gas velocity was set at zero. The initial volume fraction of the dispersed phase was also specified.
- At the inlet, a continuous phase inlet type was set. The mixture boundary condition at the outlet was specified as pressure normal flow.
- Along the wall, a no slip condition was set for the continuous phase. For the dispersed phase, a slip condition was applied.

In the case of the acoustic fluidized bed where the acoustic excitation was simulated in conjunction with the CFD model, in addition to the previous conditions, the following are the initial and boundary conditions used in the Linearized Euler model (aeroacoustics):

- The initial values of density, velocity field and pressure were all set to zero.
- A rigid wall was used in all the external boundaries of the reactor
- At the outlet, a pressure boundary condition was applied to represent the loudspeaker.

In order to apply the acoustic excitation to the fluidized bed, the acoustic field was applied at the upper boundary of the model (the outlet). To represent the acoustic vibrations of the loudspeaker, a pressure function was implemented in the model based on the experimental values of frequency and sound pressure level (Iturralde, 2016):

$$P = P_{fs} \cos \omega t \quad (17)$$

Where  $P_{fs}$  is the source amplitude and it was calculated as follows (Comsol, 2015):

$$P_{fs} = P_{ref} 10^{L_p/20} \quad (18)$$

And the angular frequency  $\omega$  was found with the following expression (Inman, 2014):

$$\omega = 2\pi f \quad (19)$$

Finally, the following expression was used at the outlet pressure boundary condition in the acoustic model of Comsol:

$$P = 6.324 \cos(1256.6)t \quad (20)$$

When both physics were simulated, the Euler-Euler model was first computed in order to use some of its variables in the acoustic model. The multiphysics coupling was done by adding the absolute pressure and velocity field of the continuous phase calculated in the Euler-Euler model, in the background mean flow pressure and background mean flow velocity of the Linearized Euler model of aeroacoustics. Likewise, the density of

the continuous phase of the CFD model was used in the acoustic model. At the moment of computing the complete model, the solvers and variables of each physics were fully coupled and solved in the same study (time dependent).

Table 1 summarizes the computational parameters and conditions applied in the current simulations for the three particle diameters analyzed.

**Table 1. Parameter values in the numerical simulations**

Parameter	Description	Value
$U_g$ (m/s)	Superficial gas velocity	0.12
$D$ (m)	Reactor diameter	0.102
$Rh$ (m)	Reactor height	0.91
$H$ (m)	Static bed height	0.102
$\rho_a$ (kg/m <sup>3</sup> )	Density, air	1.2
$\rho_g$ (kg/m <sup>3</sup> )	Density, ground walnut shell	1440
$\mu_a$ (Pa·s)	Dynamic viscosity, air	$1.8 \times 10^{-5}$
$d$ (μm)	Particle diameter	80, 150, 212
$\phi_d$	Initial concentration, dispersed phase	0.57
$F$ (Hz)	Frequency	200
$L_p$ (dB)	Sound pressure level	110
$Re_p$	Particle Reynolds number	0.729
$Re_c$	Continuous phase Reynolds number	816

The two parameters of frequency and sound pressure level were only used in the acoustic fluidized bed model with particle diameter of 212 μm, which is the model compared with experimental results.

The phase properties specified in the Euler-Euler two fluid model of Comsol were the following:

- Viscosity Model: Krieger type model
- Drag Model: Gidaspow
- Solid Pressure Model: Gidaspow-Ettehadieh

The following table shows the meshing setup used in the CFD and Acoustics simulations:

**Table 2. Meshing parameters**

<b>Particle Mesh</b>	<b>80 <math>\mu\text{m}</math> (CFD)</b>	<b>150 <math>\mu\text{m}</math> (CFD)</b>	<b>212 <math>\mu\text{m}</math> (CFD)</b>	<b>212 <math>\mu\text{m}</math> (Multiphysics)</b>
Type	Extremely fine	Extremely coarse	Extra coarse	Extremely coarse
# of elements	203738	1891	2520	1584
Grid type	Triangular (domain) Quadrilateral (boundaries)	Triangular (domain) Quadrilateral (boundaries)	Triangular (domain) Quadrilateral (boundaries)	Triangular (domain) Quadrilateral (boundaries)

For the case of the particle of 80  $\mu\text{m}$ , in the CFD simulation a time step of 0.1 s with 12 iterations per time step was used. In the CFD simulation of the particle of 150  $\mu\text{m}$ , a time step of 0.01 s with 200 iterations per time step was specified. With the particle of 212  $\mu\text{m}$ , a time step of 0.1 s with 120 iterations per time step was used (CFD analysis). On the other hand, for the multiphysics case, a time step of 0.01 s with 15 iterations per time step was chosen until convergence was reached.



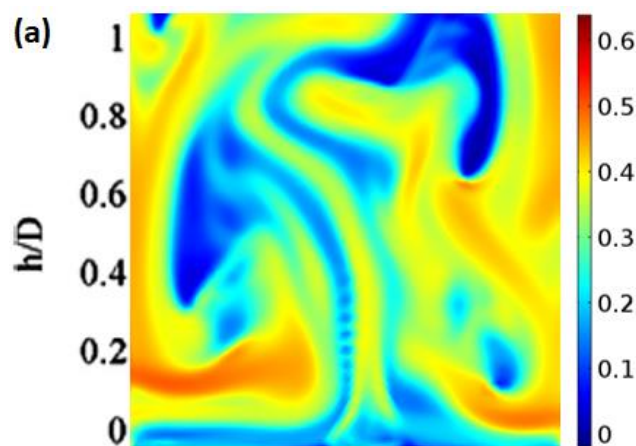
## Results and Discussion

The results of this study are classified in qualitative and quantitative results for the three particle diameters analyzed. Then, a comparison of these results with experimental data obtained previously in investigations carried out by Escudero (2014) is presented. Solid concentration maps are shown specifically for a bed height-to-diameter ratio  $h/D = 1$ , for both cases: non-acoustic condition (CFD only) and acoustic condition (Multiphysics).

### Qualitative Results

#### *Solid concentration maps (CFD)*

The solid concentration maps presented below allow to observe the qualitative characteristics of the fluidized bed in the CFD simulations (no acoustic intervention). As shown in figure 3, the hydrodynamic characteristics of the bed vary as the particle diameter increases.



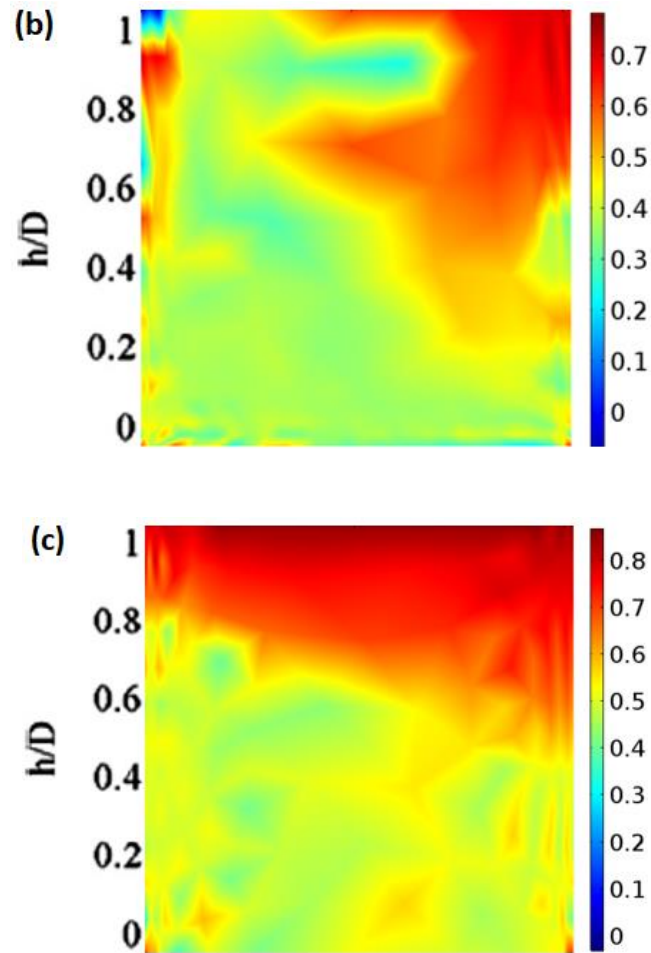


**Figure 3. Solid concentration for (a) 80  $\mu\text{m}$ , (b) 150  $\mu\text{m}$  and (c) 212  $\mu\text{m}$  ground walnut shell**

In part (a) of figure 3, it can be seen that there is more concentration of solids near the walls and also in the lower part of the bed. It can also be seen there are two main regions in which there is no presence of solids, which are represented by blue, and allows to conclude that in those regions only the presence of the continuous phase exists. On the other hand, in part (b) there is a different hydrodynamic behavior from the previous one. It can be observed that the solid particles are concentrated mainly in the upper right part of the bed. In the lower region and near the walls, the fluidization of the particles is more uniform, which is why there are no red colored areas. In the 212  $\mu\text{m}$  particles (part c), the concentration of the dispersed phase is maximum in the

upper part of the bed. From the middle region downwards, the concentration of solids is uniform and remains so, even near the walls.

### ***Solid concentration maps (Multiphysics)***

The solids concentration map of the following figure shows the hydrodynamic behavior of the fluidized bed for the multiphysics case (with acoustic intervention). This image shows the distribution of the dispersed phase inside the bed with different colors which represent different values of solids concentration.

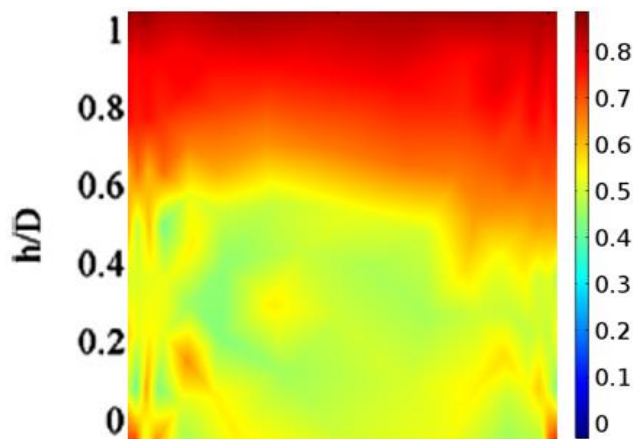
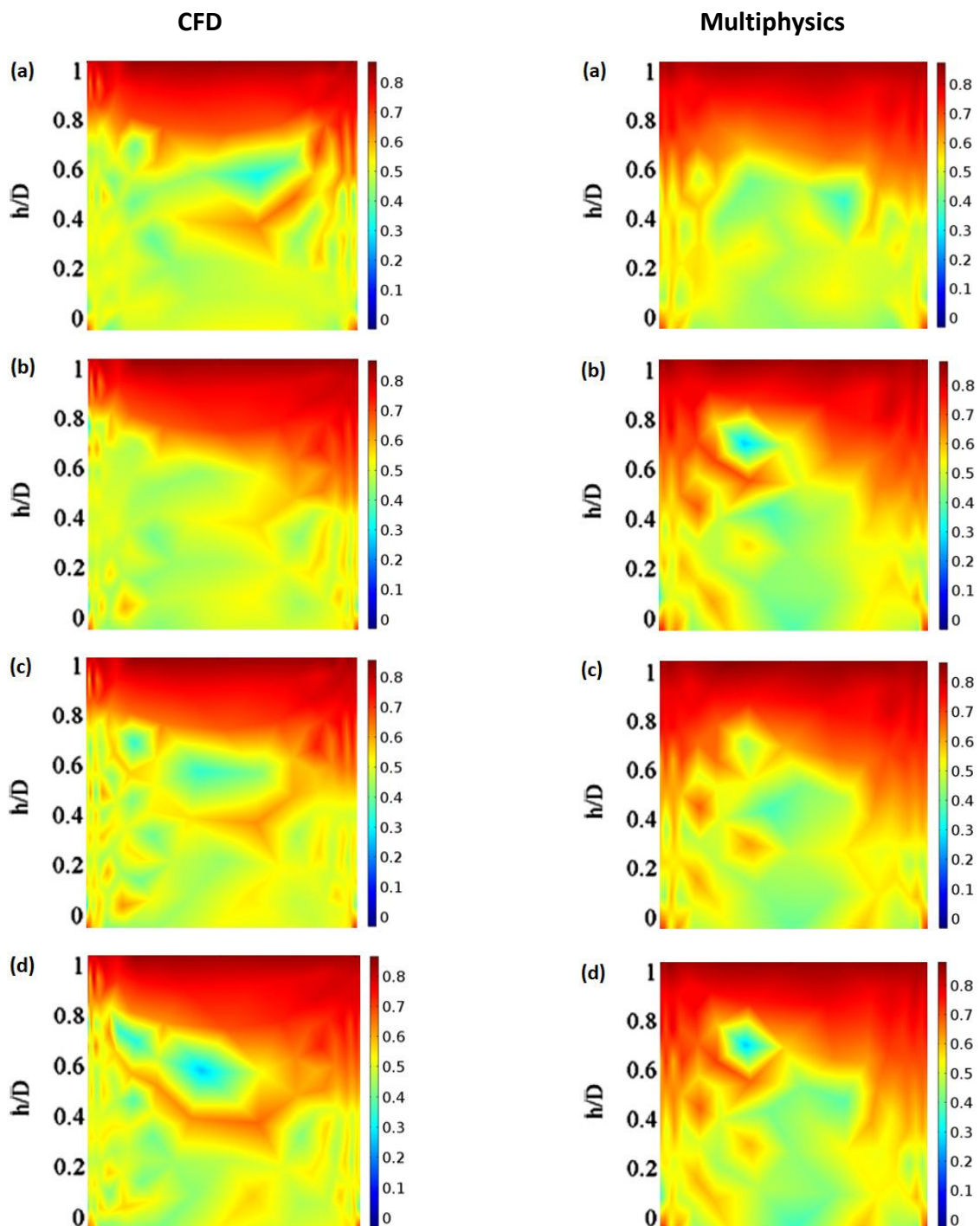


**Figure 4. Solid concentration map for 212  $\mu\text{m}$  ground walnut shell with acoustic coupling**

As shown in figure 4, at a height of 10.2 cm, the largest number of solid particles are concentrated in the upper part of the bed. When  $h/D = 0.6$  approximately, the gas-solid mixture becomes more uniform along the diameter of the fluidized bed, and this uniformity is maintained from that point downwards. In the middle and lower region of the bed, the concentration of solids is very similar in both the walls and the center of the bed. It can also be observed, in the corners at the inlet of the bed, there are small concentrations of solids (red color) that indicate a greater particle concentration with respect to the rest of the bed.

**Solid concentration maps for 212  $\mu\text{m}$  (CFD – Multiphysics Comparison)**

In order to show the influence of the acoustic vibrations in the hydrodynamic characteristics of the fluidized bed, the following figure shows the solid concentration maps for the acoustic case (Multiphysics) and the no acoustic case (CFD) at different times of simulation.



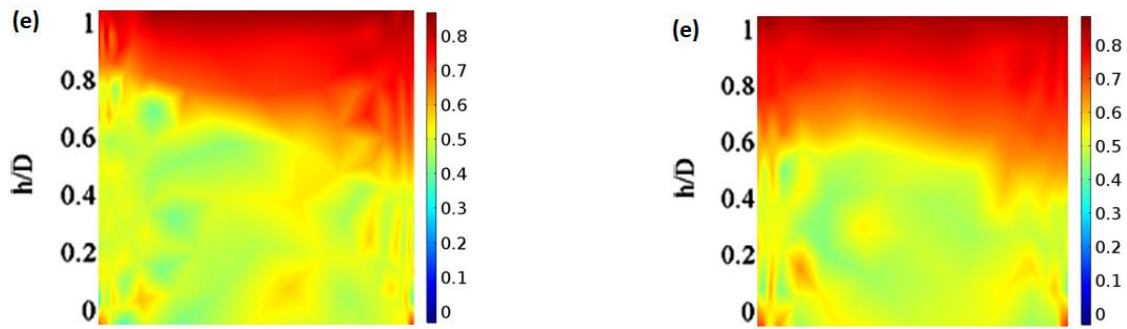


**Figure 5. Solid concentration maps for (a)  $t = 1s$ , (b)  $t = 2s$ , (c)  $t = 3s$ , (d)  $t = 4s$  and (e)  $t = 5s$**

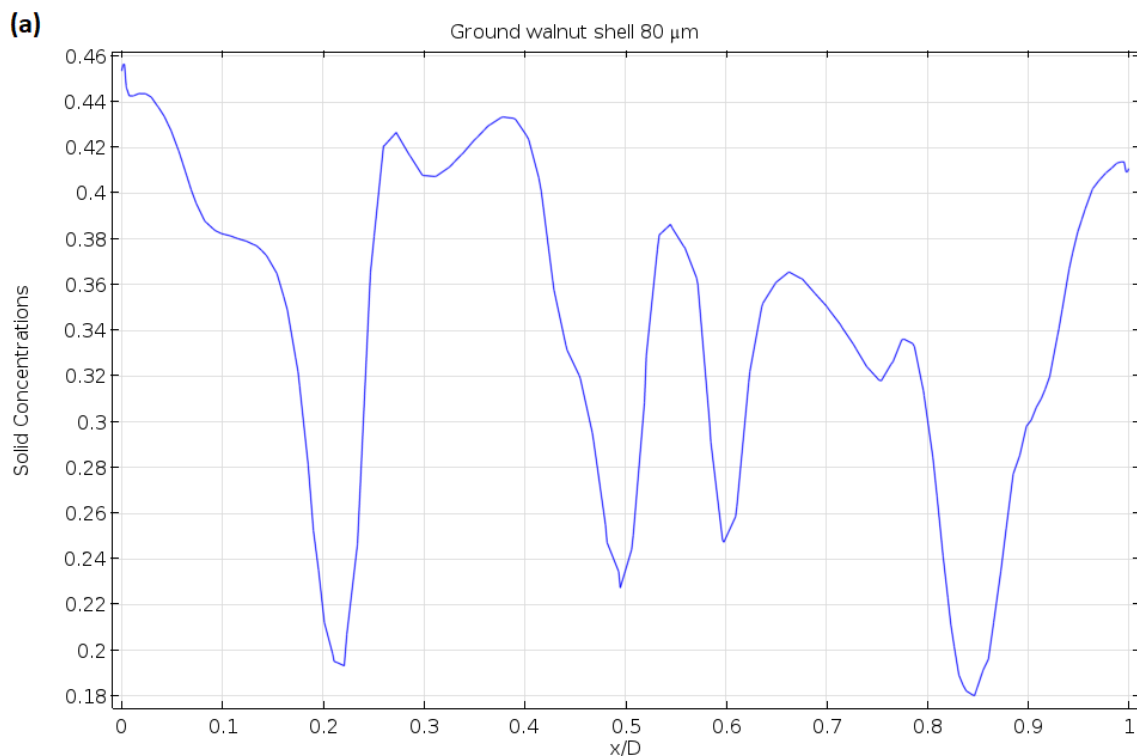
At a time of 1 second (part a), there is a difference in the solid concentration profiles between the CFD and Multiphysics cases. It can be seen from the no acoustic simulation that in the center of the bed there is a greater concentration of solid particles with respect to the other regions of the bed. This greater concentration appears at a height of  $h/D = 0.4$  approximately. When looking up the acoustic simulation at the same time of simulation, this region with higher concentration of solids disappear, and shows more uniformity in the concentration of the dispersed phase along the width of the bed. In part (b) at a time of 2 seconds, the results of the simulations show a similar hydrodynamic behavior of the solid particles inside the bed, with the difference that in the multiphysics simulation, there is more concentration of solids near the walls in the upper region of the bed. The solid concentration maps in part (c) show different gas-solid profiles especially in the middle region of the bed. It can be seen in the CFD simulation, in the center part of the bed, there is a greater concentration of particles when compared with the Multiphysics simulation. At 4 seconds of simulation (part d), at a height of  $h/D = 0.4$ , the figure shows a red colored region with high concentration of solids in the simulation with no acoustic intervention. Conversely, at the same height, this red colored region disappears when the acoustic excitation is applied, the gas-solid mixture inside the bed is more uniform

and for this reason it can be said that the fluidization process is enhanced when the acoustic vibrations are used in the system. Part (e) of figure 5, shows a better fluidization of the solid particles and a better uniformity along the width of the bed in the acoustic simulation. The CFD simulation shows a higher concentration of solids in the upper right region of the bed (near the wall). On the other hand, in the Multiphysics simulation, the solids concentration is pretty similar in both walls.

## Quantitative Results

### *Solid concentration profiles (CFD)*

The solids concentration is plotted as a function of height to determine quantitatively the variation of the dispersed phase concentration through the entire bed. The following figures are shown specifically for a bed height-to-diameter ratio  $h/D = 0.25$ .



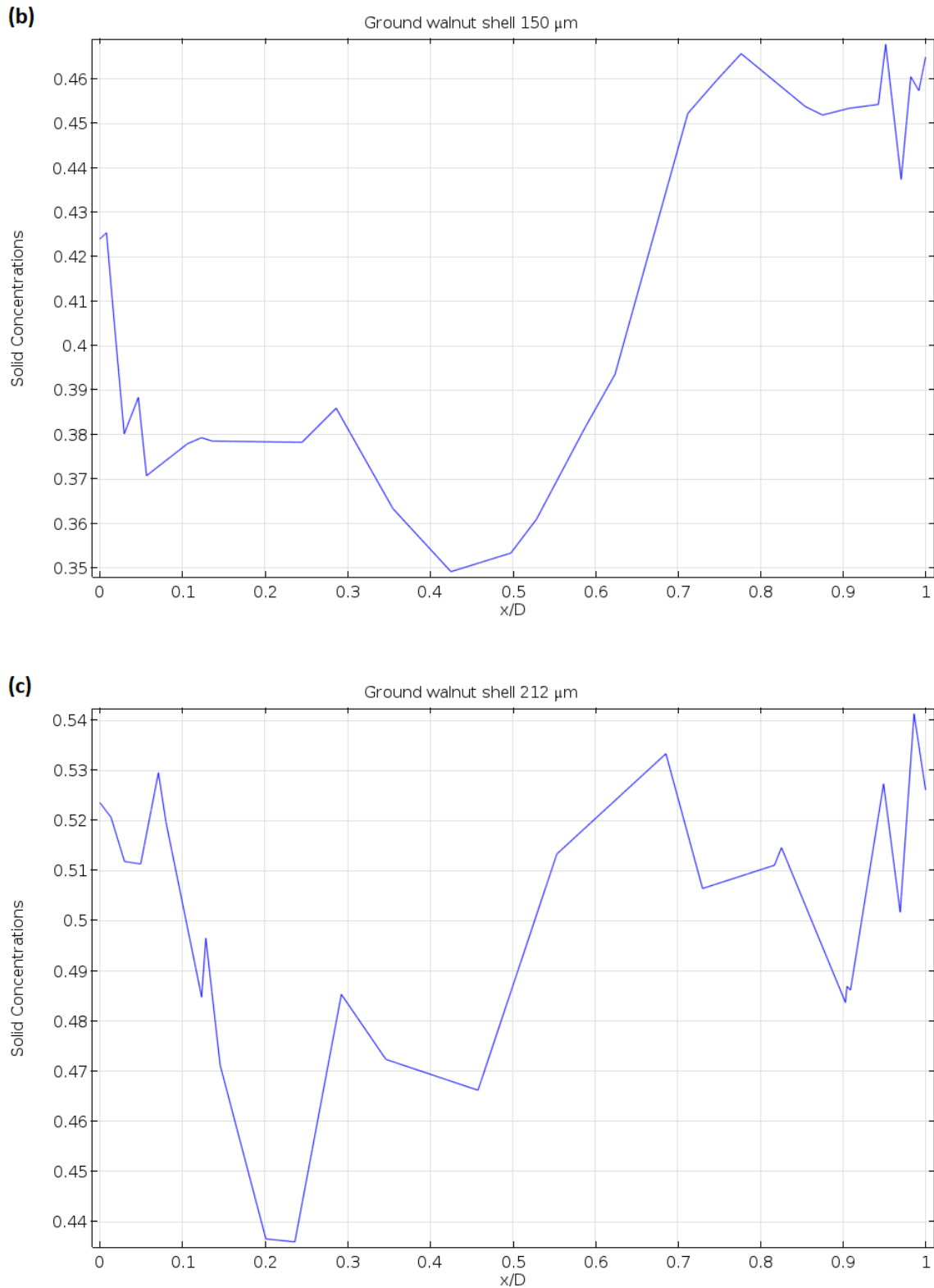


**Figure 6. Solid concentrations at a height of 2.5 cm for (a) 80  $\mu\text{m}$ , (b) 150  $\mu\text{m}$  and (c) 212  $\mu\text{m}$**

In part (a) of figure 6, it can be seen that the walnut shell concentration reaches higher values near the walls of the bed. When  $x/D$  is between 0.2 and 0.3, the solids

concentration has the lowest values, and this also happens when  $x/D$  is between 0.8 and 0.9. This decrease in solids concentration means that the continuous phase (air) is flowing in those regions. In the center of the bed width there is also an important presence of air flowing, which is the reason that the particles concentration has a low value. In part (b) with particle diameter of  $150\ \mu\text{m}$ , it can be observed that the lowest values of solids concentration are located in the center of the bed ( $x/D = 0.4$  and  $0.5$ ). Conversely, near the walls is where the higher values of solid particle concentration are shown in the figure, especially the right wall where the solids concentration reaches a maximum value with respect to the rest of the bed. The CFD simulation in part (c), shows the walnut shell concentration along the width of the bed. Near the walls of the bed, the solids concentration has higher values when compared them with the values present in the center of the bed. It is important to notice that the highest value of particles concentration is located near the right wall of the bed and the lowest value is shown to appear at  $x/D = 0.2$  approximately, which means that the presence of air in this region is greater than the other parts of the fluidized bed. The higher values of the continuous phase in this region produces a decrease in the number of particles present, and that is why this part of the figure shows lower values of solids concentration inside the bed.

### ***Solid concentration profiles (Multiphysics)***

The solids concentration plot of the following figure shows quantitatively the hydrodynamic behavior of the fluidized bed for the multiphysics case (with acoustic intervention) for the ground walnut shell with particle diameter of  $212\ \mu\text{m}$ .



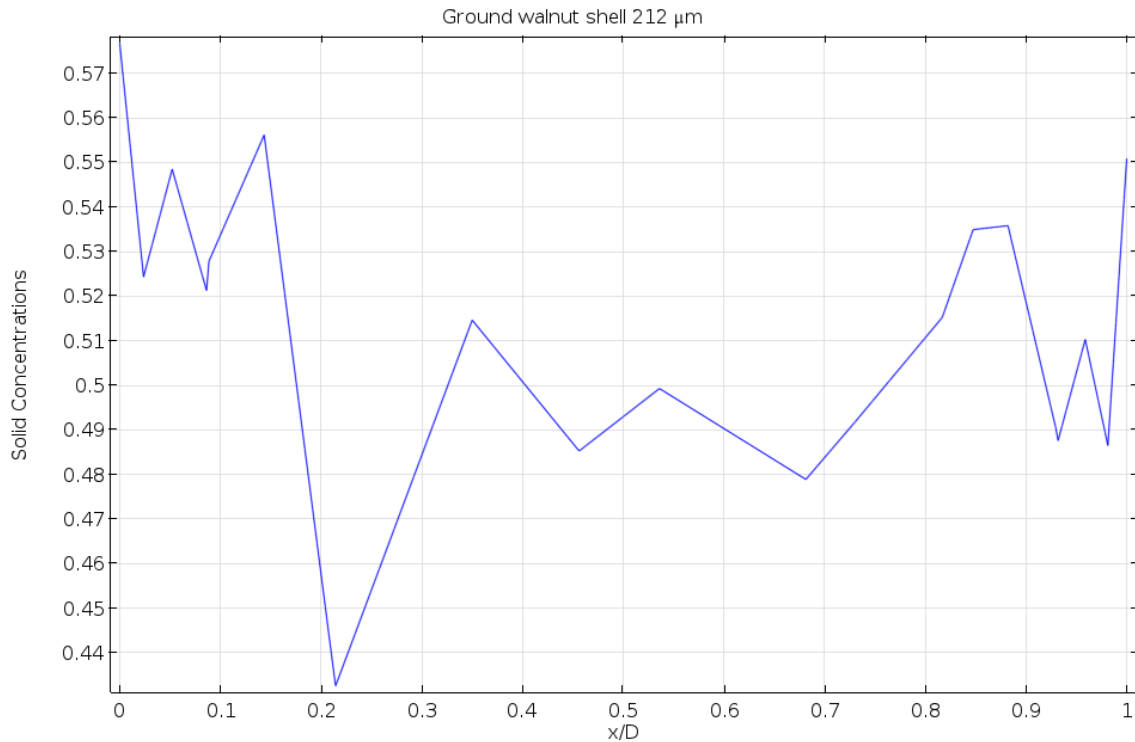


**Figure 7. Solid concentrations at a height of 2.5 cm for 212  $\mu\text{m}$  at  $t = 5\text{s}$**

It is observed in figure 7 that the concentration of solids across the width of the bed is more uniform mainly in the center of the bed. It can also be observed that in the walls of the bed, the concentration of solids increases with respect to the central part. At approximately  $x/D = 0.2$ , the concentration of the dispersed phase reaches the lowest values of this graph, in other words, the gas holdup in this region has maximum values.

#### ***Solid concentration profiles for 212 $\mu\text{m}$ (CFD – Multiphysics Comparison)***

The following plots were taken at a simulation time of 5 seconds in order to show the influence of the acoustic vibrations in the hydrodynamic behavior of the fluidized bed. Both graphs show the solid concentration profiles of ground walnut shell at a bed height-to-diameter ratio  $h/D = 0.25$ .

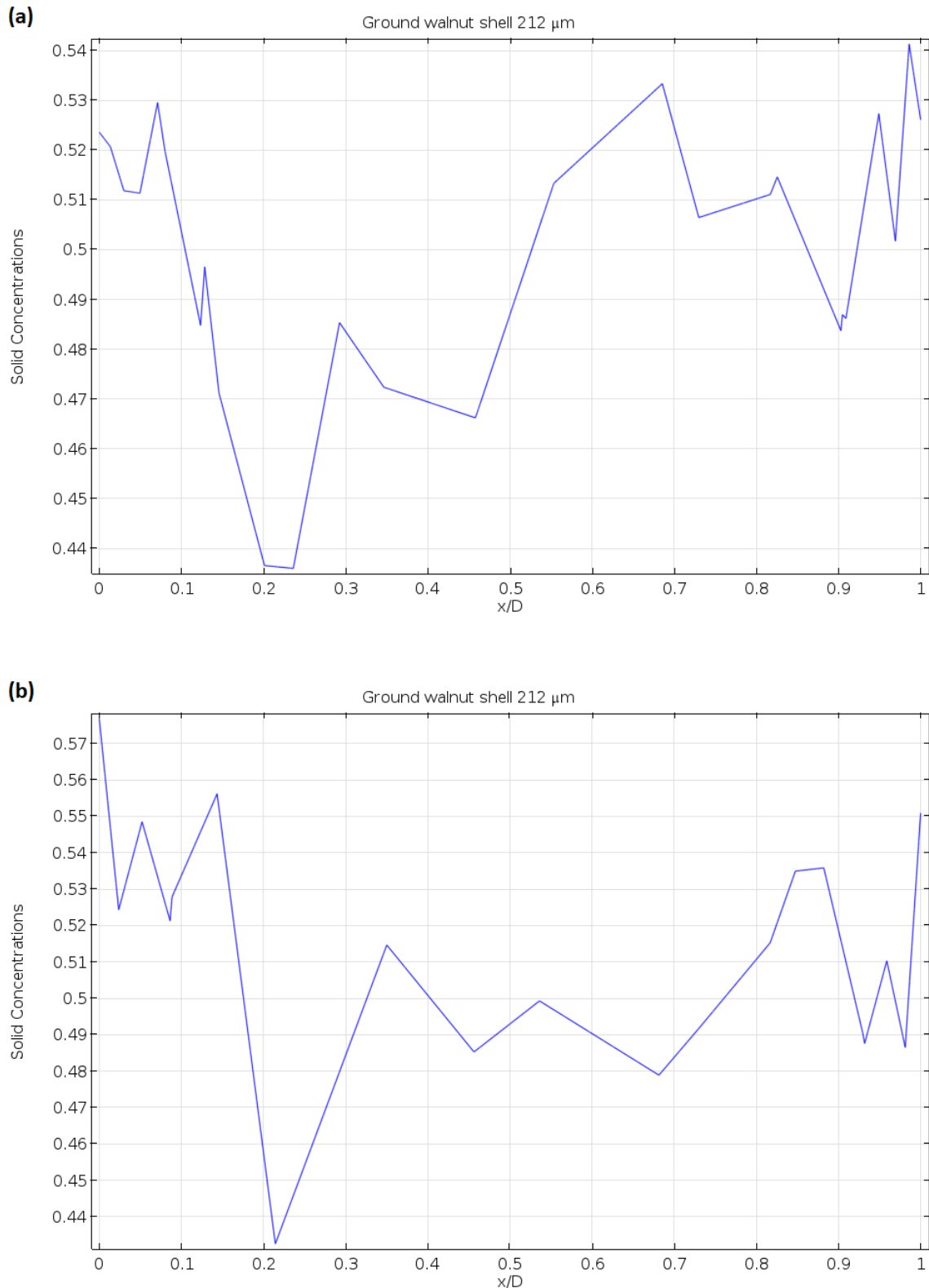


**Figure 8. Solid concentrations at a height of 2.5 cm for (a) CFD and (b) Multiphysics at  $t = 5\text{s}$**

In part (a) of figure 8, the solids concentration along the width of the bed shows a fairly changeable trend throughout. Near the walls of the bed, the walnut shell

concentration reaches higher values when compared them with the values present in the center of the bed. It is important to notice that the highest value of solids concentration is located in the right wall of the bed and the lowest value is shown between  $x/D = 0.2$  and  $0.3$  approximately, which means that the presence of the continuous phase in this region is greater with high values of gas holdup. In the region between  $x/D = 0.2$  and  $0.5$ , the lower values of the dispersed phase mean an increase in the gas holdup, and that is why this part of the graph shows low values of solids concentration inside the bed. In part (b), it can be seen a different trend of the curve when the acoustic excitation is applied in the fluidized bed. The concentration of walnut shell across the diameter of the bed is more uniform and has more constant values of concentrations. It can also be observed that in the walls of the bed, the concentration of solids increases with respect to the central region. By having more constant values of concentrations, it can be said that the fluidization inside the bed has been improved in a certain way. In both graphs, specifically between  $x/D = 0.2$  and  $0.3$ , the concentration of solid particles reaches the minimum values of each curve.

### **Comparison with experimental results**

In order to make a comparison between the numerical model with the experimental data, all the experimental conditions used remained the same in the present simulations (Escudero, 2014): A 10.2 cm diameter fluidized bed, ground walnut shell as the solid particles, particle diameter of  $212 \mu\text{m}$ , same frequency and sound pressure level (200 Hz and 110 dB) and  $U_g = 3U_{mf}$

### Qualitative results

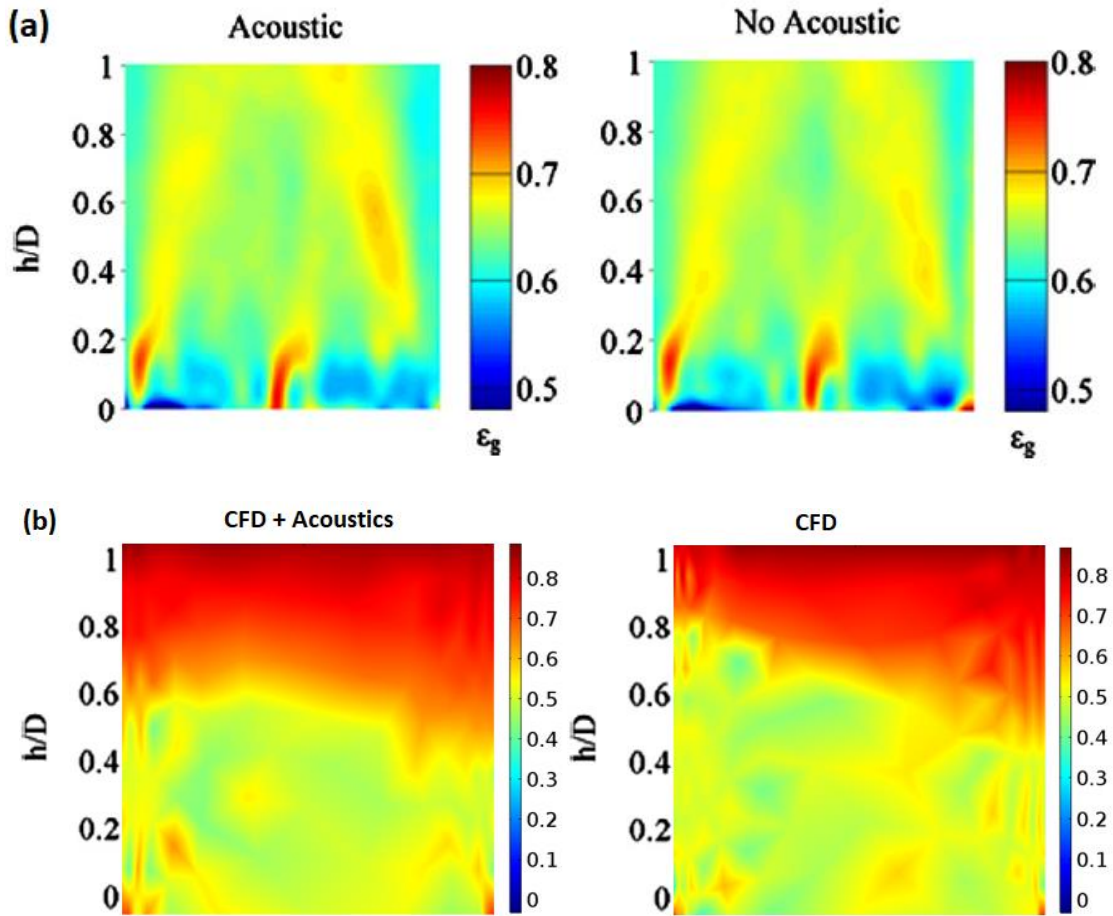


Figure 9. Qualitative comparison between (a) experimental data (gas holdup) and (b) numerical results (solids concentration) for 212  $\mu\text{m}$  walnut shell

Experimentally, two-dimensional time-average local gas holdup maps were obtained to show the qualitative characteristics of the acoustic effects in the fluidized bed (Escudero, 2014). In part (a) of figure 9 these experimental maps are shown for the acoustic and no acoustic cases. On the other hand, in the numerical simulations, solid concentration maps ( $\phi_d = 1 - \phi_c$ ) are shown in part (b) of figure 9 for both cases, the multiphysics study and the CFD study. It can be seen from the CFD results that there is a high concentration of solids in the upper region of the bed. It can also be observed, there is more solids concentration near the right wall when compared with the left

wall of the bed. In other words, we can conclude that there is not much uniformity in the solids concentration along the diameter of the bed, specifically near the top of the bed. The solid concentration map of the multiphysics case (with acoustic intervention), shows a small difference when comparing it with the CFD case (no acoustics). In the middle region of the bed, the fluidization of the solid particles shows a more uniform pattern with less voids. In both walls, the concentration of solids is pretty similar and it can be seen that the solids volume fraction along the diameter of the bed has more uniformity specially in the middle region of the bed, so that, it can be concluded that the acoustic field improves the fluidization process, which can be seen in the experimental results where the acoustic intervention produced a more uniform void fraction distribution.

It should be noted that in the lower part of the bed of the experimental maps, different profiles are shown when comparing them with those of the simulations. This is due to the fact that the air inlet in the experimental reactor had a series of small holes. On the other hand, in the numerical simulations, these holes were represented as a single air inlet in the computational model.

### ***Quantitative results***

Local time-average gas holdup is plotted in the experimental results. Solid concentrations are plotted in the numerical simulations at a time of 5 seconds and at a height of  $h = 2.5$  cm. The experimental curves for the acoustic and no acoustic cases are plotted in the same figure, while the curves of the numerical simulations are plotted in separate figures.

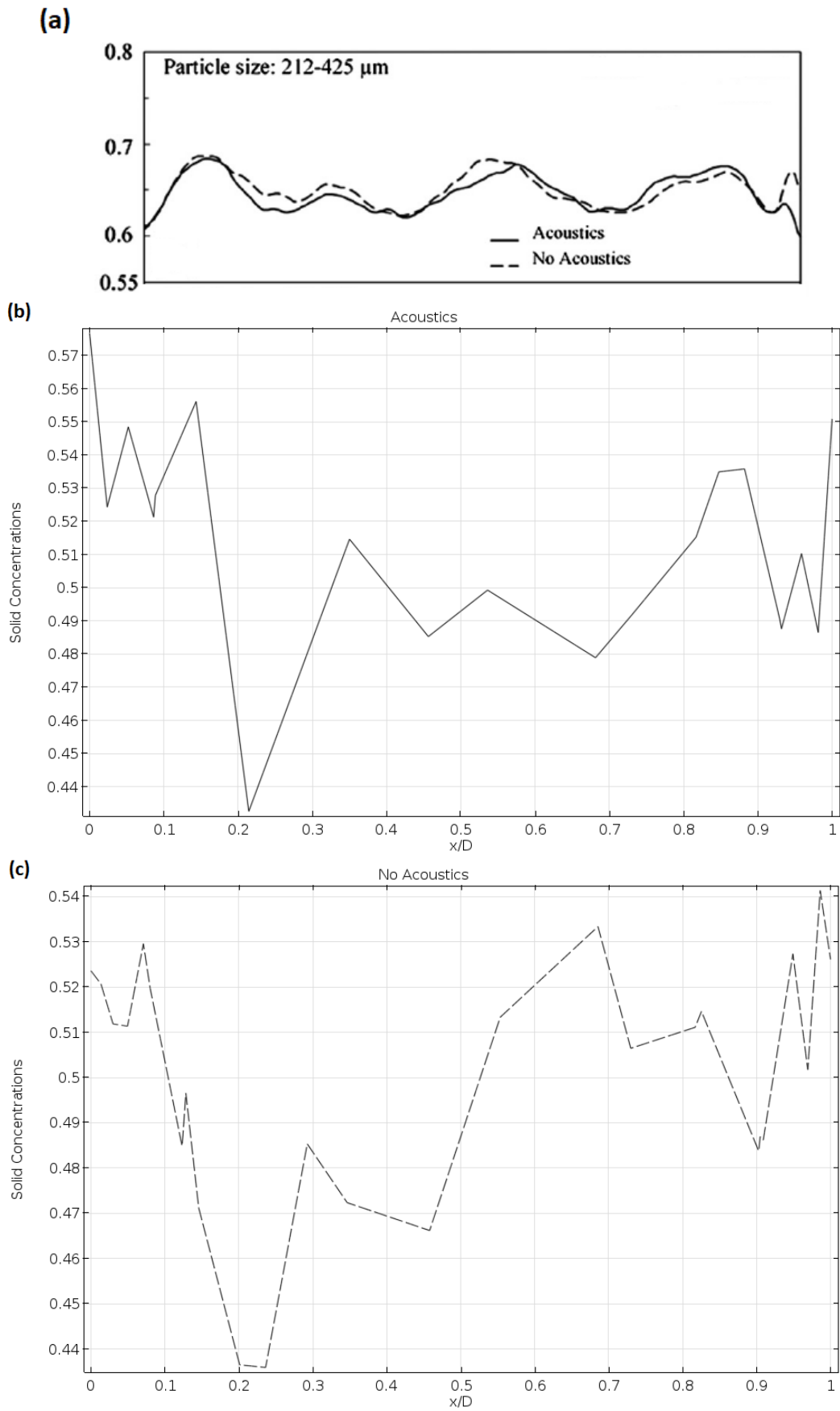


**Figure 10. Quantitative comparison between (a) experimental data (gas holdup), (b) numerical results (acoustics) and (c) numerical results (no acoustics) for 212  $\mu\text{m}$  walnut shell**

The experimental data of figure 10 shows a slight difference between the acoustic and no acoustic cases. Both lines follow a very similar pattern showing a small influence of the acoustic field in the fluidization of the bed. When comparing part (b) and (c) of figure 10, it can be seen a difference between the acoustic and no acoustic cases. At a height of 2.5 cm, the multiphysics simulation (acoustics) shows a more uniform concentration of solids when comparing it with the CFD case (no acoustics). In part (b), between  $x/D = 0.1$  and  $0.2$ , the solids concentration reaches a maximum value and the minimum value of concentration is shown to be between  $x/D = 0.2$  and  $0.3$ . A similar trend can be seen in part (c) where the lowest value of particles concentration is between  $x/D = 0.2$  and  $0.3$ , the difference is that in the no acoustics simulation, the maximum value of solids concentration is located near the right wall of the bed.

The presence of acoustic vibrations inside the bed, allows the curve of part (b) to have more constant values of solids concentration, that is, there are not sudden changes in the concentration values as can be seen in part (c). This trend can be noted especially in the central region of the bed. As seen in the two graphs obtained from the numerical simulations for both cases, CFD (no acoustics) and multiphysics (acoustics), the acoustic excitation does not have significant effects on the hydrodynamic behavior of the fluidized bed for this type and size of particle. This can be confirmed with the results obtained experimentally (part a), since the curves plotted in the figure do not show an important change between the acoustic and non-acoustic cases.

## Conclusions

Comsol Multiphysics simulated successfully the hydrodynamic behavior of an acoustic fluidized bed reactor. In order to accomplish this, a 2D computational model of a gas-solid fluidized bed was implemented, in which the coupling of the CFD module with the acoustics one allowed the modeling of the reactor, the solution of the governing equations and obtaining results of the hydrodynamic behavior of the system.

The effects of frequency and sound pressure level in the hydrodynamics of the fluidized bed reactor model were determined. To do so, the Euler-Euler two fluid model was fully coupled with the Linearized Euler model of aeroacoustics to obtain solid concentrations for particles of Geldart type A and B analyzed in this study. The value of frequency of 200 Hz and sound pressure level of 110 dB used experimentally, remained the same in the present simulations for ground walnut shell with particle diameter of 212  $\mu\text{m}$ .

The computational model, qualitative and quantitative data from the simulations were compared and validated with experimental results. Gas holdup maps obtained experimentally showed that the acoustic intervention improved the fluidization behaviour of the gas-solid flow. Solid concentration maps resulted from the numerical simulations, showed more uniformity along the diameter of the bed when adding the acoustic field. It can be concluded from the experimental and numerical data that a fluidized bed assisted by acoustic excitation exhibits a more uniform fluidization and the hydrodynamic structure of this multiphase system is enhanced.



## References

- Comsol. (2015). The CFD Module User's Guide. *Comsol Guide*.
- Comsol. (2015). The Acoustics Module User's Guide. *Comsol Guide*.
- Cloete, S., Johansen, S. T., & Amini, S. (2014). Grid independence behaviour of fluidized bed reactor simulations using the Two Fluid Model: Effect of particle size. *Powder Technology*, 269, 153–165. <https://doi.org/10.1016/j.powtec.2014.08.055>
- Escudero, D., & Heindel, T. J. (2013). Minimum fluidization velocity in a 3D fluidized bed modified with an acoustic field. *Chemical Engineering Journal*, 231, 68–75. <https://doi.org/10.1016/j.cej.2013.07.011>
- Escudero, D. R., & Heindel, T. J. (2014). Acoustic fluidized bed hydrodynamics characterization using X-ray computed tomography. *Chemical Engineering Journal*, 243, 411–420. <https://doi.org/10.1016/j.cej.2014.01.025>
- Fan, R. (2006). *Computational fluid dynamics simulation of fluidized bed polymerization reactors*. (Doctoral Thesis). Iowa State University, Ames, Iowa.
- Inman, D. (2014). *Engineering Vibration*. New Jersey: Pearson.
- Iturralde, G. (2016). *Acoustic Standing Waves Modelling in Gas Solid Fluidized Beds*. San Francisco de Quito University, Quito, Ecuador.
- Khosravi Bizhaem, H., & Basirat Tabrizi, H. (2017). Investigating effect of pulsed flow on hydrodynamics of gas-solid fluidized bed using two-fluid model simulation and experiment. *Powder Technology*, 311, 328–340. <https://doi.org/10.1016/j.powtec.2017.01.027>
- Patro, B. (2014). *Eulerian modeling of gas-solid multiphase flow in horizontal pipes*. (Master Thesis). National Institute of Technology Rourkela, Odisha, India.
- Shah, M. T., Utikar, R. P., & Pareek, V. K. (2017). CFD study: Effect of pulsating flow on gas–solid hydrodynamics in FCC riser. *Particuology*, 31, 25–34. <https://doi.org/10.1016/j.partic.2016.07.002>
- Shuai, W., Xiang, L., Huilin, L., Guodong, L., Jiaying, W., & Pengfei, X. (2011). Simulation of cohesive particle motion in a sound-assisted fluidized bed. *Powder Technology*, 207(1–3), 65–77. <https://doi.org/10.1016/j.powtec.2010.10.011>
- Wu, G., Ouyang, J., Yang, B., Li, Q., & Wang, F. (2012). Lagrangian-Eulerian simulation of slugging fluidized bed. *Particuology*, 10(1), 72–78. <https://doi.org/10.1016/j.partic.2011.07.003>

Zhang, K., Zhang, J., & Zhang, B. (2003). Experimental and numerical study of fluid dynamic parameters in a jetting fluidized bed of a binary mixture. *Powder Technology*, 132(1), 30–38. [https://doi.org/10.1016/S0032-5910\(03\)00041-X](https://doi.org/10.1016/S0032-5910(03)00041-X)